



**Physicochemical properties of "Green"-Nanocrystalline
Cellulose isolated from recycled newspaper**

Journal:	<i>RSC Advances</i>
Manuscript ID:	RA-ART-12-2014-017020.R1
Article Type:	Paper
Date Submitted by the Author:	26-Feb-2015
Complete List of Authors:	Mohamed, Mohamad Azuwa; Universiti Teknologi Malaysia, Advanced Membrane Technology Research Centre (AMTEC); Universiti Teknologi Malaysia, Faculty of Petroleum & Renewable Energy Engineering Wan Salleh, Wan Norharyati; Universiti Teknologi Malaysia, Advanced Membrane Technology Research Centre (AMTEC); Universiti Teknologi Malaysia, Faculty of Petroleum & Renewable Energy Engineering Jaafar, Juhana; Universiti Teknologi Malaysia, Advanced Membrane Technology Research Centre (AMTEC); Universiti Teknologi Malaysia, Faculty of Petroleum & Renewable Energy Engineering Mohd Asri, Syazeven Effatin Azma; Universiti Teknologi Malaysia, Department Chemistry, Faculty of Science Ismail, Ahmad Fauzi; Universiti Teknologi Malaysia, Advanced Membrane Technology Research Centre (AMTEC); Universiti Teknologi Malaysia, Faculty of Petroleum & Renewable Energy Engineering

ARTICLE

Physicochemical properties of “Green”-Nanocrystalline Cellulose isolated from recycled newspaper

Cite this: DOI: 10.1039/x0xx00000x

M.A. Mohamed,^{a,b} W. N. W. Salleh,^{a,b} J. Jaafar,^{a,b} S. E. A. M. Asri^c, and A. F. Ismail^{a,b}Received 00th January 2012,
Accepted 00th January 2012

DOI: 10.1039/x0xx00000x

www.rsc.org/

“Green” nanocrystalline cellulose (NCC) was isolated through acid hydrolysis process from recycled newspapers and prepared from the treatment with NaOH and NaClO₂. Morphological characterization and physicochemical properties were executed using scanning electron microscopy (SEM), atomic force microscopy (AFM), transmission electron microscopy (TEM), Fourier transform infrared (FTIR) spectroscopy, x-ray diffraction (XRD), and thermogravimetric analysis (TGA). FTIR and chemical composition analysis demonstrated that lignin and hemicellulose structures were removed using different steps of pre-treatment with NaOH and NaClO₂. From the results of SEM, it was discovered that the size of fibril of purified cellulose reduced to a great extent, and the structure of cellulose microfibril became smoother and cleaner due to the removal of lignin with other extractives. The results of XRD analysis revealed that NCC exhibits the highest crystallinity index after acid hydrolysis of bleached cellulose microfibrils. TEM and AFM analysis revealed that the rod-like structure of NCC was obtained with the size of 5.78 ± 2.14 nm wide and 121.42 ± 32.51 nm in length. The results of TGA suggested that the thermal stability of the NCC was affected mainly by the dehydration reaction caused by sulphate groups. The isolated nanocrystalline cellulose attracts great interest as an inexpensive bio-based fillers in polymer nanocomposites.

Introduction

Nowadays, the utilization of commercially available plastics and synthetic polymers has become popular among researchers. However, before the revolution of synthetic polymers, mankind and natures used natural polymers to make life possible. Due to environmental concerns and awareness that petroleum resources are finite, the use of biodegradable polymers produced from renewable resources has increased significantly. Examples of polymers from renewable resources include natural polymers such as cellulose, chitin, and starch.¹ Cellulose is the world's most abundant natural occurring polymer and can be isolated from plants and microorganisms. Cellulose is a linear homopolymer of glucose (C₆H₁₀O₅)_n with repeating units consisting of D-glucose in ⁴C₁ conformation, insoluble in water, and fully biodegradable by microbes and fungal enzymes.² Renewable semi-crystalline natural polymers including cellulose consist both amorphous and crystalline structures but it will not melt upon heating because of its crystalline region. The amorphous region can be removed by acid hydrolysis process.³⁻⁹

Nowadays, the application of nanocrystalline cellulose (NCC) as a biodegradable material has grown rapidly in

nanotechnology industry. However, there are some disadvantages of NCC including not commercially available and time consuming in its production, which limits its application in wide range of fields.¹⁰ Petersson et al. (2007) successfully produced an NCC treatment using *tert*-butanol-chloroform solvent exchange method.¹¹ The properties of cellulose acetate butyrate (CAB) nanocomposite in NCC solvent exchange have been studied by Etang et al (2009).¹² As reported, the thermal stability of the composite increased with the increase of solvent exchange content in both studies.

Haafiz et al. (2014) reported a comparative study of physicochemical and thermal properties of NCC as determined by FTIR, SEM, XRD and TGA analyses.⁶ A nanoscale structure of NCC was analysed using TEM. SEM images of the NCC showed that the structure was found to be broken down after the treatment. A study on the morphology and thermal properties of polylactic acid (PLA) reinforced NCC was previously reported.¹³ The NCC produced through acid hydrolysis process resulted in nanofibers of 60-160 nm in length and of 10-20 nm in thickness as proved by SEM.

In recent years, there has been wide interest in production of cellulose from various resources such as jute, ramie and

bagasse fibres. This work focuses on the isolation of nanocrystalline cellulose (NCC) from recycled newspaper. This approach would be an environmental friendly act since tonnes of newspapers are discarded every year. Furthermore, the production of NCC from recycled newspaper would provide a green approach to newspaper recycling and cost-effective. The NCC was prepared through acid hydrolysis process using sulphuric acid. The surface morphology of the NCC was studied using scanning electron microscopy (SEM), transmission scanning electron microscopy (TEM), and atomic force microscopy (AFM), whereas the crystallinity index of the produced NCC was studied by x-ray diffraction (XRD). The thermal properties of the materials were investigated using thermogravimetric analysis (TGA).

Experimental

Materials

Non-printed area of recycled newspaper was used as cellulose source. Sodium hydroxide pellets, sulphuric acid (95-97 %), and nitric acid (65 %) were purchased from QReC. Sodium chlorite (80 %) was purchased from Sigma Aldrich. All the chemicals were reagent grade and were used as received.

Extraction of cellulose from newspaper

Small pieces of old newspaper were grounded with a grinder. First, alkali treatment was applied to the ground old newspaper. 20 g of ground newspaper was added to 800 mL of 5 wt% NaOH solution and mixed homogeneously until a green mixture was obtained. The mixture was boiled at 125 °C for 2 h under constant, continuous mechanical stirring. As the boiling process was completed, the sample was washed with distilled water until a neutral pH was achieved. The cellulose extraction was continued by NaClO₂ treatment. Few drops of 60 wt % HNO₃ were added dropwise into 800 mL of 2 w/v % NaClO₂ solution. Then, the sample was added into the NaClO₂ solution under vigorous and continuous mechanical stirring at 125 °C for 2 h. The NaClO₂ treatment was repeated until a white sample was obtained.

Isolation of nanocrystalline cellulose

NCC was prepared by acid hydrolysis method. First, the prepared cellulose was added to 65 wt % H₂SO₄ solution at 45 °C. Hydrolysis time in this study was fixed at 60 min, which was found to be the optimum time. The ratio of the obtained cellulose to liquor was 5:100 (wt %). The hydrolysis process of cellulose sample was stopped by adding 4-5 times cold distilled water. The diluted suspension was washed 5 times by centrifugation (5,000 rpm and 15 min) to obtain precipitates and remove excess sulphuric acid. The suspension was then dialyzed against distilled water until a constant pH was reached.

The resulting suspension was sonicated for 30 min. Then, the suspension was overnight in an oven at 65 °C.

Characterization

Determination of chemical composition of fibers

The cellulose, hemicellulose and lignin of the RNP and chemically treated fibers was determined according to A.Sonia et al. (2013).¹⁴ The holocellulose (cellulose + hemicelluloses) content was determined according to the method described in TAPPI 249-75. The α -cellulose content of the fibers was then determined by T203-99. The difference between the values of holocellulose and α -cellulose gives the hemicelluloses content of the fibers. The lignin content was analyzed by reaction with 72 % H₂SO₄ using acid insoluble lignin calculation. A minimum of three samples from each material was tested, and the averaged values were obtained as shown in **Table 1**.

Fourier transform infrared spectroscopy (FTIR)

Fourier transform infrared (FTIR) spectra were obtained from a Perkin Elmer infrared spectrometer using attenuated total reflection (ATR) accessory to provide non-destructive measurement method. All samples were in direct contact with ATR diamond by clamping the sample to the diamond surface, and pressure was applied to ensure good optical contact between the sample and the diamond. All samples were scanned within the wave range of 650 – 4000 cm⁻¹.

Morphological structure analysis

The surface morphology and pore size distribution of the samples were studied by using scanning electron microscopy (SEM) and atomic force microscopy (AFM). SEM was carried out using Hitachi scanning electron microscope at an acceleration voltage of 15 kV. The samples were sputter coated with gold to avoid charging. AFM measurement was performed using XE-100 Park System, an atomic force microscope with SSS-NCHR non-contact probes at 1 μ m/s of scan speed. The dimensions of the prepared samples were obtained from transmission electron microscopy (TEM) PHILIPS CM12 at an accelerating voltage of 100 kV.

X-ray diffraction (XRD)

The crystallinity of samples was determined by Siemens X-ray diffractometer D5000 with CuK α radiation of wavelength 0.15406 nm at 40 kV and 40 mA. The diffracted intensity was measured by scanning range of $2\theta = 20 - 80^\circ$ with a step speed of 2 $^\circ$ /min. The crystallinity of the samples was calculated from diffraction intensity data using the empirical method for native cellulose. The crystalline-to-amorphous ratio material was determined using Eq. (1).

$$\text{Cr.I (\%)} = \frac{1002 - I_{am}}{1002} \quad (1)$$

Where $C_r I$ is the crystallinity index, I_{002} is the maximum intensity (in arbitrary units) of the diffraction from 002 plane at $2\theta = 22.6^\circ$, and I_{am} is the intensity of the background scatter measured at $2\theta = 19^\circ$.¹⁵ The crystal sizes were estimated using Scherrer equation (Eq. (2)).

$$D_{hkl} = \frac{0.9 \lambda}{\beta_{1/2} \cos \theta} \quad (2)$$

Where D_{hkl} is the crystal dimension perpendicular to diffracting planes with Miller indices of hkl , λ is the wavelength of X-ray radiation ($\lambda = 0.15406 \text{ \AA}$) and $\beta_{1/2}$ is the full width at half maximum (FWHM) of the diffraction peaks.^{4,16}

Surface Charge

The surface charge of prepared NCC was determined by conductometric titration method as described by previous study.^{17,18} 45 mL of the 0.01 % NCC suspensions was mixed with 5 mL of 0.01M NaCl. The mixture was stirred for 5 min before the measurements. The aqueous NaOH solution (0.1 M) was added dropwise with continuous stirring. The change in conductivity was recorded by a conductometer after each step.

Thermogravimetric analysis (TGA)

Thermal stability of the samples was characterized using thermogravimetric analysis (TGA). Dry sample was ground into fine powder and the sample was placed in a platinum pan. The analysis was carried out at a heating rate of $10^\circ\text{C}/\text{min}$ over $20 - 600^\circ\text{C}$ temperature range under air atmosphere.

Results and Discussion

FTIR spectroscopy analysis

FTIR spectra of raw newspaper (RNP), cellulose microfiber treated by NaOH (CMF-NaOH), cellulose microfiber treated by NaClO_2 (CMF- NaClO_2), and NCC are illustrated in **Fig. 1**. Based on the FTIR spectra, all samples showed identical absorption band, which indicates that all samples have similar chemical compositions. Two main absorbance regions can be observed in **Fig. 1**. These regions are found at high wavenumber (2800 cm^{-1}) and at low wavenumber ($800-1700 \text{ cm}^{-1}$). The peaks at 1595 , 1505 , and 1247 cm^{-1} in RNP spectrum are associated to the characteristic of lignin. Small shoulder peak at 1595 cm^{-1} is attributed to the C=C unsaturated linkages, aromatic rings present in lignin.¹⁹ The peak at 1505 cm^{-1} refers to the aromatic C=C in plane symmetrical stretching of aromatic ring present in lignin.^{20,21} Moreover, the peak at 1247 cm^{-1} is attributed to the C-O of guaiacyl unit stretching vibration in lignin.¹⁹ After RNP had undergone NaOH treatment, the peak at 1595 cm^{-1} has almost disappear and the intensity of 1505 cm^{-1} was reduced. Interestingly, after the sample was further treated with NaClO_2 the peak at 1505 cm^{-1} disappeared from the spectrum in **Fig. 1(c)**. This indicates that a

complete lignin removal in the samples can be achieved by NaClO_2 treatment. This result is in good agreement with the chemical composition analysis where the sample CMF- NaClO_2 exhibits lowest lignin content of 0.89 % as shown in the **Table 1**. Previous study suggested that the main characteristic peak of hemicellulose can be observed around $1728 - 1731 \text{ cm}^{-1}$.^{16,22,23} However, this peaks are absent in the all samples. Other important peak that related to hemicellulose characteristic can be observed at $1245 - 1249 \text{ cm}^{-1}$ which is assigned to acyl-oxygen CO-OR stretching vibration in hemicellulose.^{19,14} The peak at 1247 cm^{-1} in RNP sample has sharply decreased after alkaline treatment indicating the removal of hemicellulose.

The spectral band at $3333-3500 \text{ cm}^{-1}$ refers to the O-H stretching vibration of OH group.²⁰ A previous study also suggests that this spectral band refers to the O-H stretching of intramolecular hydrogen bond for cellulose I.³ The peak observed at $2890-2918 \text{ cm}^{-1}$ is due to C-H stretching.²⁴ The spectra of all samples in the region of $1639-1645 \text{ cm}^{-1}$ are due to O-H bending as fiber absorbed water.^{24,25} Although all FTIR samples were subjected to proper drying process, the elimination of water from fiber was very difficult. This may be due to the cellulose-water interaction. The occurrence of spectral band at 1428 cm^{-1} for all samples is due to CH_2 asymmetric bending motion in cellulose.²⁶ In addition, previous study also suggests that the presence of this peak is due to intermolecular hydrogen attraction at C6 group.¹⁵ The spectral band observed at $1370-1375 \text{ cm}^{-1}$ is due to C-H bending or asymmetric C-H deformation,¹⁴ $1315-1316 \text{ cm}^{-1}$ is due to CH_2 wagging,²⁷ 1163 cm^{-1} is due to C-O anti-symmetric stretching,²⁸ and $1104-1105 \text{ cm}^{-1}$ is due to C-O and C-C stretching.²⁶ The sharp peak observed at 1030 cm^{-1} is due to C-O and C-C stretching.^{26,27} The C-O-C pyranose ring stretching vibration gives obvious band at $1053-1054 \text{ cm}^{-1}$.²⁰ The increase in the intensity of the band $1053-1054 \text{ cm}^{-1}$ shows the increase in the cellulose contents.²² The increment of cellulose content after chemical treatments can be observed in **Table 1**. The band at 897 cm^{-1} in the FTIR spectrum shows typical cellulose structure associated with the cellulosic β -glycosidic linkages that consist of C₁-H and O-H bending.^{6,15,22,14} The vibrational assignments are summarized in **Table 2**.

Table 1: Chemical compositions of RNP, CMF-NaOH and CMF- NaClO_2 .

Table 2: FTIR absorption band for RNP, CMF-NaOH, and CMF- NaClO_2 , and NCC.

Fig. 1: FTIR spectra of recycled newspaper during isolation process: (a) RNP as a raw material, (b) CMF-NaOH, (c) CMF- NaClO_2 , and (d) NCC after acid hydrolysis.

Morphological structure studies

Scanning electron microscopy (SEM) analysis

The surface morphology of cellulose microfibril was observed by scanning electron microscopy (SEM). **Fig. 2(a), 2(b), and 2(c)** shows different colour of pulp before and after the treatment. Definitely, after the treatment, the colour of the extracted cellulose from RNP as a raw material changed from slightly grey to slightly yellow, and finally, white cellulose pulp was obtained. The alkaline treatment was designed to solubilise any other extractives and hemicelluloses residual in the RNP samples. The solubilised components were washed out with water, leaving a slightly yellow residue of cellulose and lignin as shown in **Fig. 2(b)**. Previous study suggested that, the slightly yellow colour is corresponded to the presence of lignin within the fibers.²⁹ The delignification treatments with acidified sodium chlorite was performed to break down phenolic compounds or molecules having chromophoric group present in lignin and to remove the by-product of such breakdown, to whiten the pulp as shown in the **Fig. 2 (c)**.^{22,14} Throughout the treatment, the cellulose became highly purified since after the addition of NaClO₂, the surface of cellulose microfibril became smoother and cleaner, which confirmed the removal of lignin with other extractives after delignification with acidified sodium chlorite as shown as in **Fig. 2(f)**.^{14,30,31}

It can also be seen that there is a reduction in the diameter and size of fibril of purified cellulose to a great extent due to the removal of lignin with some other extractives as shown in **Fig. 2(d), 2(e), and 2(f)** for comparison purpose. Similar observation of reduction in diameter and size also can be found elsewhere.²⁵ The average final diameter of fibril of purified cellulose was approximately $7.7 \pm 2.3 \mu\text{m}$.

Fig. 2: Pictures and SEM images of (a), (d) RNP as a raw material, (b), (e) CMF-NaOH, and (c), (f) CMF-NaClO₂.

Atomic force microscopy (AFM)

The dimension of the produced NCC was elucidated by AFM. An air dried, highly diluted suspension (0.001 w/w %) deposited on freshly cleaved mica surface. **Fig. 3** shows AFM images of the produced NCC prepared by different steps of chemical pre-treatments and followed by acid hydrolysis. Nanoscale rod-like structure or needle-like structure were observed in AFM 3D and height view.

The produced nanorod shape of NCC revealed that acid hydrolysis of long cellulose microfibril could cleave the amorphous region of microfibrils into bundles of nanocrystalline cellulose, resulting in a dimension reduction of fiber from micron to nanometer.^{25,30} Thus, it has been discovered that the highly uniform nanorod NCC with an average dimension size of $23.7 \pm 15.1 \text{ nm}$ was obtained as portrayed in **Fig. 3 (c)**.

Fig. 3: AFM images of NCC: (a) 3D view, (b) height view, and (c) lateral size distribution.

Transmission electron microscopy (TEM)

TEM is considered as a powerful technique to obtain more insight into the morphological structure of the produced NCC. The presence of highly uniform nanorod or needle-like shape of the produced NCC was further confirmed by TEM observations as shown in **Fig. 4**. The average size distribution of the produced NCC was analyzed and found to be $5.78 \pm 2.14 \text{ nm}$ wide and $121.42 \pm 32.51 \text{ nm}$ in length. This dimension is considered lower than the dimension reported for NCC isolated from raw cotton linter and sugarcane bagasse.^{3,20,32} It can be observed that the NCC particles aggregated to some extent in TEM images probably due to the evaporation of water. Similar observation can also be found elsewhere.¹⁷

Fig. 4: TEM images of NCC from acid hydrolysis.

X-ray diffraction studies

The crystallinity of RNP-pulp, CMF-NaOH, CMF-NaClO₂, and NCC was analyzed using XRD technique. The x-ray diffractograms in Fig 5 present cellulose I crystal diffraction pattern peaks around $2\theta = 14.8^\circ, 16.4^\circ, 22.6^\circ,$ and 34.6° , corresponding to the (101), (110), (200), and (040) crystal planes respectively.²⁰ The diffraction peak at 22.6° became sharper and narrower from RNP-pulp to NCC. This indicates higher perfection of crystal lattice in (200) plane.^{4,28}

The crystallinity index and crystalline dimension of RNP, CMF-NaOH, CMF-NaClO₂, and NCC can be observed in **Table 3**. The crystallinity index of the samples increased as it undergone different steps of chemical pretreatment of NaOH and NaClO₂ followed by acid hydrolysis.¹⁶ The increase in crystallinity can be attributed to the removal of lignin during NaOH and NaClO₂ pretreatment.²² Furthermore, the appearance of weak diffraction peak at (040) revealed the removal of most of the lignin and hemicellulose from RNP-pulp.²⁸ Moreover, the peak at 14.8° and 16.4° became more intense, indicating a more compact and ordered crystalline structure especially in NCC diffraction peak. The increase of the degree in crystallinity of the NCC is due to removal of amorphous region in the cellulose chain during acid hydrolysis. The crystallinity index for RNP, CMF-NaOH, CMF-NaClO₂, and NCC were 82.0 %, 84.24 %, 88.46 %, and 90.15 %, respectively.

The average crystalline dimension of RNP-pulp was 4.89 nm and those for CMF-NaOH, CMF-NaClO₂, and NCC were 4.96 nm, 5.24 nm, and 5.70 nm, respectively. The average crystalline dimension of NCC is in agreement with those obtained from TEM. The increase in crystalline dimension of NCC mainly reflects the narrowing of the crystallite size distribution after acid hydrolysis process.¹⁶ Thus, it can be concluded that the crystallite sizes increased as the diffraction peak became sharper and narrower.

Fig 5: XRD pattern of RNP-pulp, CMF-NaOH, CMF-NaClO₂, and NCC

Table 3: Crystallinity index and crystalline dimension of RNP-Pulp, CMF-NaOH, CMF-NaClO₂, and NCC.

Surface Charge

This analysis was done to study the existent of sulfate group on the surface of isolated NCC. The higher surface charge indicates a greater incorporation of sulfate groups into the NCC produced from sulphuric acid hydrolysis.¹⁸ Furthermore, the higher surface charge promotes a stable NCC suspension with good dispersibility in aqueous system.⁴ As shown the Fig. 4 (c), the produced NCC with 153 ± 14 $\mu\text{mol/g}$ surface charge exhibited good dispersion in water. This surface charge is comparable with one (148 ± 11 $\mu\text{mol/g}$) obtained from bio-residue from wood bioethanol production.¹⁸ This was due to the existing of sulphate groups on the surface of NCC which leading to the electrostatic repulsion between NCC particles.³³

Thermogravimetric analysis

In this study, thermogravimetric analysis (TGA) was carried out in the effort to investigate the thermal properties of RNP-Pulp, CMF-NaOH, CMF-NaClO₂ and NCC. The results from the TGA are graphically presented in Fig. 6, which shows the relationship between weight percentage (%) and temperature for all the produced materials. The thermal degradation data ($T_{5\%}$), ($T_{20\%}$), ($T_{50\%}$), the residual weight at 600 °C and the peak degradation temperature (T_{max}) are listed in Table 4.

It can be concluded from Fig. 6 that all materials are thermally stable in the region below 170 °C. From the TGA and DTG curves, all materials showed initial weight loss at the region between 100 °C and 150 °C. The weight loss occurs due to the evaporation of moisture content or any other volatile matters inside the samples.^{11,34} The TGA curve also shows that NCC started to undergo a degradation step earlier compared to RNP-Pulp, CMF-NaOH, and CMF-NaClO₂. This is due to the deposition of sulphate group during acid hydrolysis process. In the isolation process, the use of H₂SO₄ resulted in the presence of sulphate groups on NCC particles.¹⁷ The thermal stability of NCC is affected mainly due to dehydration reaction caused by sulphate groups.¹⁸

According to Table 4, it is interesting to state that NCC possesses the highest residues at 600 °C compared to RNP-Pulp, CMF-NaOH, and CMF-NaClO₂. This behaviour is also probably caused by the introduction of sulphate groups during hydrolysis, and sulphate acts as a flame retardant by promoting dehydration reactions. At the same time, sulphate groups are also suspected to reduce thermal stability.³⁵

Fig 6: TGA and DTG curves of (a) CMF-NaClO₂, (b) CMF-NaOH, (c) RNP-pulp and (d) NCC.

Table 4: Thermal stability data of RNP-pulp, CMF-NaOH, CMF-NaClO₂, and NCC

Conclusions

In this paper, green and sustainable nanocrystalline cellulose (NCC) was produced from the utilization of recycled newspaper. The yield of NCC was about 54.6 % when the sulfuric acid concentration is 65 %, reaction temperature is 45 °C and the hydrolysis time is 1 h. From the analysis of scanning electron microscopy (SEM), the size of fibril of purified cellulose reduced significantly due to the removal of lignin with some other extractives. AFM and TEM studies give supporting evidences for the formation rod-like structure of NCC. It was found that the size of NCC after acid hydrolysis (65 wt % H₂SO₄ at 45 °C for 1 h) was 5.78 ± 2.14 nm wide and 121.42 ± 32.51 nm in length. The thermal stability of the produced NCC was affected mainly due to the dehydration reaction caused by the sulphate groups from acid hydrolysis process. The obtained NCC has the possibility to be used as nanocomposites with enhanced properties.

Acknowledgements

The authors would like to thank Universiti Teknologi Malaysia (UTM), Ministry of Higher Education Malaysia (MOHE) and Research University Grant (05H08) for the facilities and financial support.

Notes and references

- ^a Advanced Membrane Technology Research Centre, Universiti Teknologi Malaysia, 81310 Skudai, Johor Bahru, Malaysia.
^b Faculty of Petroleum and Renewable Energy Engineering, Universiti Teknologi Malaysia, 81310 Skudai, Johor Bahru, Malaysia.
^c Department of Chemistry, Faculty of Science, Universiti Teknologi Malaysia, 81310 Skudai, Johor Bahru, Malaysia.

1. L. Yu, K. Dean, and L. Li, *Prog. Polym. Sci.*, 2006, **31**, 576–602.
2. R. Li, J. Fei, Y. Cai, Y. Li, J. Feng, and J. Yao, *Carbohydr. Polym.*, 2009, **76**, 94–99.
3. A. Kumar, Y. S. Negi, V. Choudhary, and N. K. Bhardwaj, *J. Mater. Phys. Chem.*, 2014, **2**, 1–8.
4. Y. Liu, H. Wang, G. Yu, Q. Yu, B. Li, and X. Mu, *Carbohydr. Polym.*, 2014, **110**, 415–422.
5. S. Elazzouzi-hafraoui, Y. Nishiyama, J. Putaux, L. Heux, F. Dubreuil, and C. Rochas, *Biomacromolecules*, 2008, **9**, 57–65.
6. M. K. M. Haafiz, A. Hassan, Z. Zakaria, and I. M. Inuwa, *Carbohydr. Polym.*, 2014, **103**, 119–25.
7. F. Jiang and Y.-L. Hsieh, *Carbohydr. Polym.*, 2013, **95**, 32–40.
8. Y. Habibi, L. a. Lucia, and O. J. Rojas, *Chem. Rev.*, 2010, **110**, 3479–3500.

9. B. S. Lalia, E. Guillen, H. a. Arafat, and R. Hashaikeh, *Desalination*, 2014, **332**, 134–141.
10. M. Grunert and W. T. Winter, *J. Polym. Environ.*, 2002, **10**, 27–30.
11. L. Petersson, I. Kvien, and K. Oksman, *Compos. Sci. Technol.*, 2007, **67**, 2535–2544.
12. J. Etang Ayuk, A. P. Mathew, and K. Oksman, *J. Appl. Polym. Sci.*, 2009, **114**, 2723–2730.
13. M. D. Sanchez-Garcia and J. M. Lagaron, *Cellulose*, 2010, **17**, 987–1004.
14. A. Sonia and K. Priya Dasan, *Carbohydr. Polym.*, 2013, **92**, 668–74.
15. M. K. Mohamad Haafiz, S. J. Eichhorn, A. Hassan, and M. Jawaid, *Carbohydr. Polym.*, 2013, **93**, 628–34.
16. P. Lu and Y.-L. Hsieh, *Carbohydr. Polym.*, 2012, **87**, 564–573.
17. N. Wang, E. Ding, and R. Cheng, *Polymer.*, 2007, **48**, 3486–3493.
18. M. a. Herrera, A. P. Mathew, and K. Oksman, *Mater. Lett.*, 2012, **71**, 28–31.
19. C. Chen, J. Luo, W. Qin, and Z. Tong, *Monatshefte für Chemie - Chem. Mon.*, 2013, **145**, 175–185.
20. A. Mandal and D. Chakrabarty, *Carbohydr. Polym.*, 2011, **86**, 1291–1299.
21. I. Samfira, M. Butnariu, S. Rodino, and M. Butu, *Dig. J. Nanomater. Biostructures*, 2013, **8**, 1679–1686.
22. S. Elanthikkal, U. Gopalakrishnapanicker, S. Varghese, and J. T. Guthrie, *Carbohydr. Polym.*, 2010, **80**, 852–859.
23. A. I. S. Brigida, V. M. A. Calado, L. R. B. Gonçalves, and M. A. Z. Coelho, *Carbohydr. Polym.*, 2010, **79**, 832–838.
24. S. M. L. Rosa, N. Rehman, M. I. G. de Miranda, S. M. B. Nachtigall, and C. I. D. Bica, *Carbohydr. Polym.*, 2012, **87**, 1131–1138.
25. J. I. Morán, V. a. Alvarez, V. P. Cyras, and A. Vázquez, *Cellulose*, 2007, **15**, 149–159.
26. M. Szymanska-Chargot and A. Zdunek, *Food Biophys.*, 2013, **8**, 29–42.
27. M. Kacuráková, A. C. Smith, M. J. Gidley, and R. H. Wilson, *Carbohydr. Res.*, 2002, **337**, 1145–53.
28. X. Chen, J. Yu, Z. Zhang, and C. Lu, *Carbohydr. Polym.*, 2011, **85**, 245–250.
29. Wang Yueping, Wang Ge, Cheng Haitao, Tian Genlin, Liu Zheng, Xiao Qun Feng, Zhou Xiangqi, Han Xiaojun, and Gao Xushan, *Text. Res. J.*, 2010, **80**, 334–343.
30. R. M. Sheltami, I. Abdullah, I. Ahmad, A. Dufresne, and H. Kargarzadeh, *Carbohydr. Polym.*, 2012, **88**, 772–779.
31. D. Bhattacharya, L. T. Germinario, and W. T. Winter, *Carbohydr. Polym.*, 2008, **73**, 371–377.
32. J. P. S. Morais, M. D. F. Rosa, M. D. S. M. de Souza Filho, L. D. Nascimento, D. M. do Nascimento, and A. R. Cassales, *Carbohydr. Polym.*, 2013, **91**, 229–35.
33. S. J. Eichhorn, *Soft Matter*, 2011, **7**, 303.
34. E. Fortunati, D. Puglia, M. Monti, L. Peponi, C. Santulli, J. M. Kenny, and L. Torre, *J. Polym. Environ.*, 2012, **21**, 319–328.
35. M. Roman and W. T. Winter, *Biomacromolecules*, 2004, **5**, 1671–7.

Tables

Table 1: Chemical compositions of RNP, CMF-NaOH and CMF-NaClO₂

Samples	Cellulose (%)	Hemicellulose (%)	Lignin (%)
RNP	55.21	15.33	29.46
CMF-NaOH	79.58	4.42	16.00
CMF-NaClO ₂	98.7	0.28	0.89

Table 2: FT-IR absorption band for functional group of RNP, CMF-NaOH, CMF-NaClO₂ and NCC.

Peak assignment	Peak frequency (cm ⁻¹)			
	RNP	CMF-NaOH	CMF-NaClO ₂	NCC
O-H stretching	3336	3335	3333	3333
C-H stretching	2918	2890	2898	2898
O-H bending	1645	1637	1635	1635
C=C unsaturated linkages	1595	-	-	-
C=C stretching of aromatic ring	1505	1505	-	-
CH ₂ symmetric bending	1428	1428	1428	1428
C-H bending	1370	1370	1375	1375
CH ₂ wagging	1316	1316	1315	1316
C-O of guaiacyl unit stretching & Acyl-oxygen CO-OR stretching	1247	1247	-	-
C-O anti-symmetric stretching	1163	1163	1163	1163
C-O and C-C stretching	1104	1105	1104	1104
C-O-C stretching	1053	1054	1053	1053
C-O and C-C stretching	1030	1030	1030	1030
C-H	897	897	897	897

Table 3: Crystallinity index and crystalline dimension of RNP-Pulp, CMF-NaOH, CMF-NaClO₂, and NCC.

Sample	Crystallinity Index (%)	Average Crystalline Dimension (nm)
RNP-Pulp	82.00	4.89
CMF-NaOH	84.24	4.96
CMF-NaClO ₂	88.46	5.24
NCC	90.15	5.70

Table 4: Thermal stability data of RNP-pulp, CMF-NaOH, CMF-NaClO₂, and NCC

Samples	T _{5%} (°C)	T _{20%} (°C)	T _{50%} (°C)	DTG peak, T _{max} (°C)		Residue at 600 °C (%)
				T _{max1}	T _{max2}	
RNP-Pulp	252.9	305.6	340.6	346.4	-	25.3
CMF-NaOH	239.4	297.3	337.9	343.6	-	21.0
CMF-NaClO ₂	233.5	291.5	337.8	360.8	-	18.5
NCC	176.0	250.8	343.7	187.4	320.6	31.3

Figures

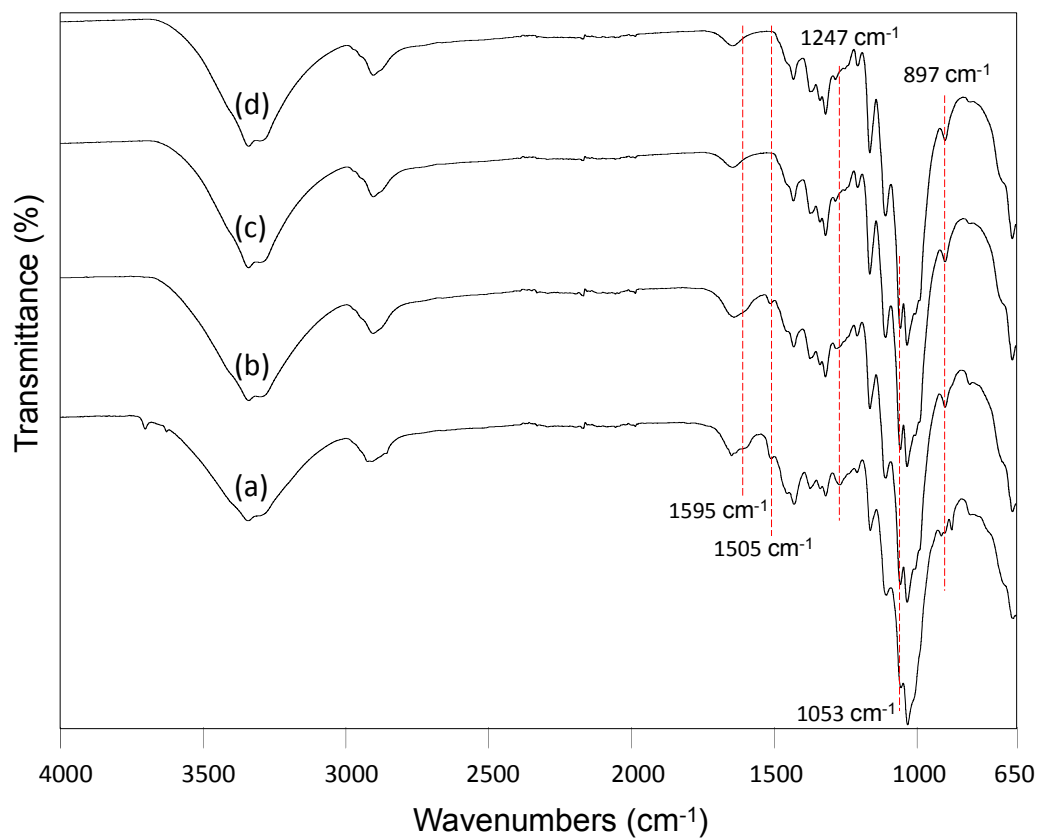


Fig 1: FTIR spectrum of recycled newspaper during isolation process: (a) RNP as raw material, (b) CMF-NaOH, (c) CMF-NaClO₂, and (d) NCC after acid hydrolysis.

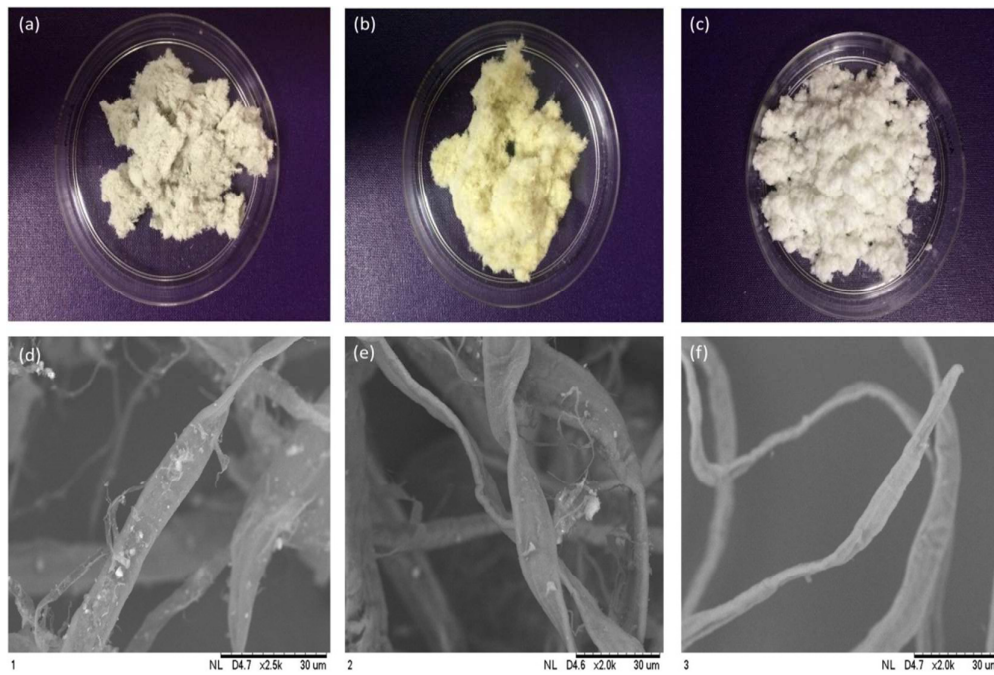


Fig. 2: Picture and scanning electron microscope image (a),(d) RNP as raw materials; (b) (e) Cellulose fiber after NaOH treatment; (c) (f) Cellulose fiber after NaClO₂ treatment.

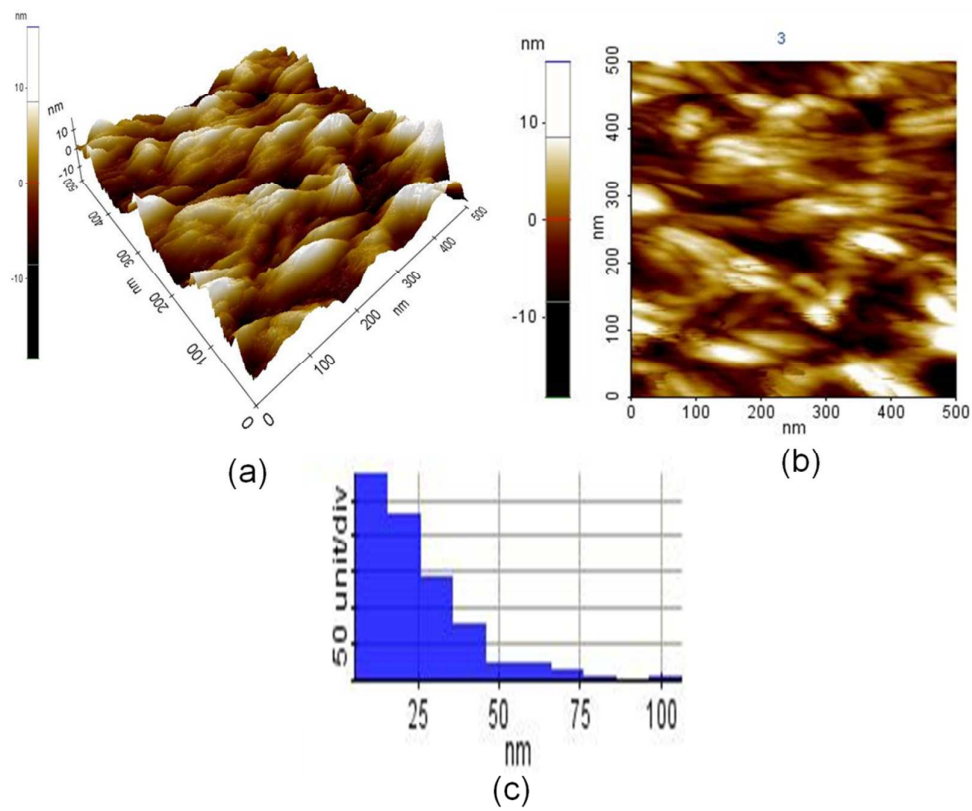


Fig 3: AFM image of NCC: (a) 3D view, (b) Height view, and (c) lateral size distribution.

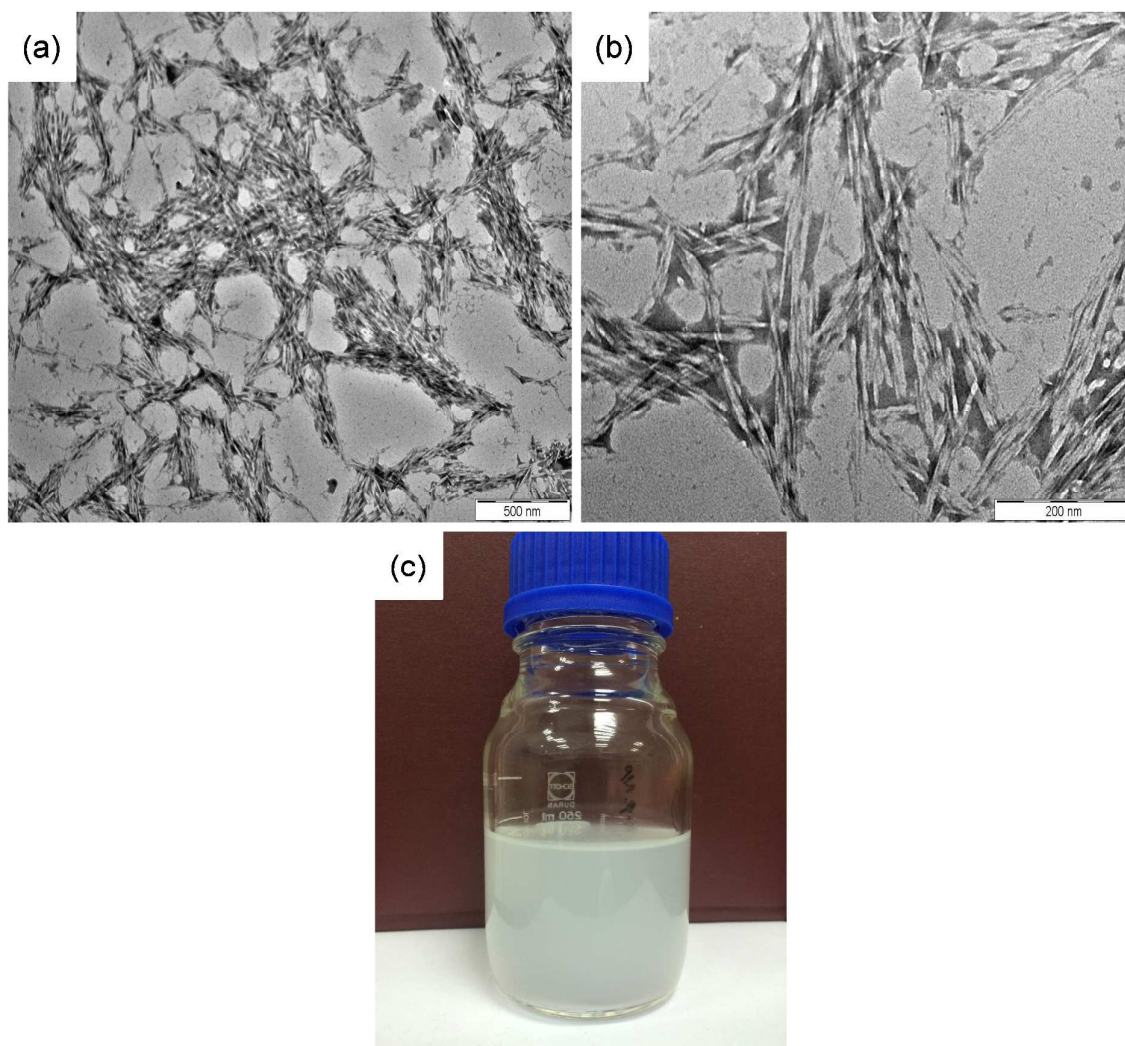


Fig 4: (a) and (b) is TEM images of NCC from acid hydrolysis and (c) photograph of dispersion of NCC in water.

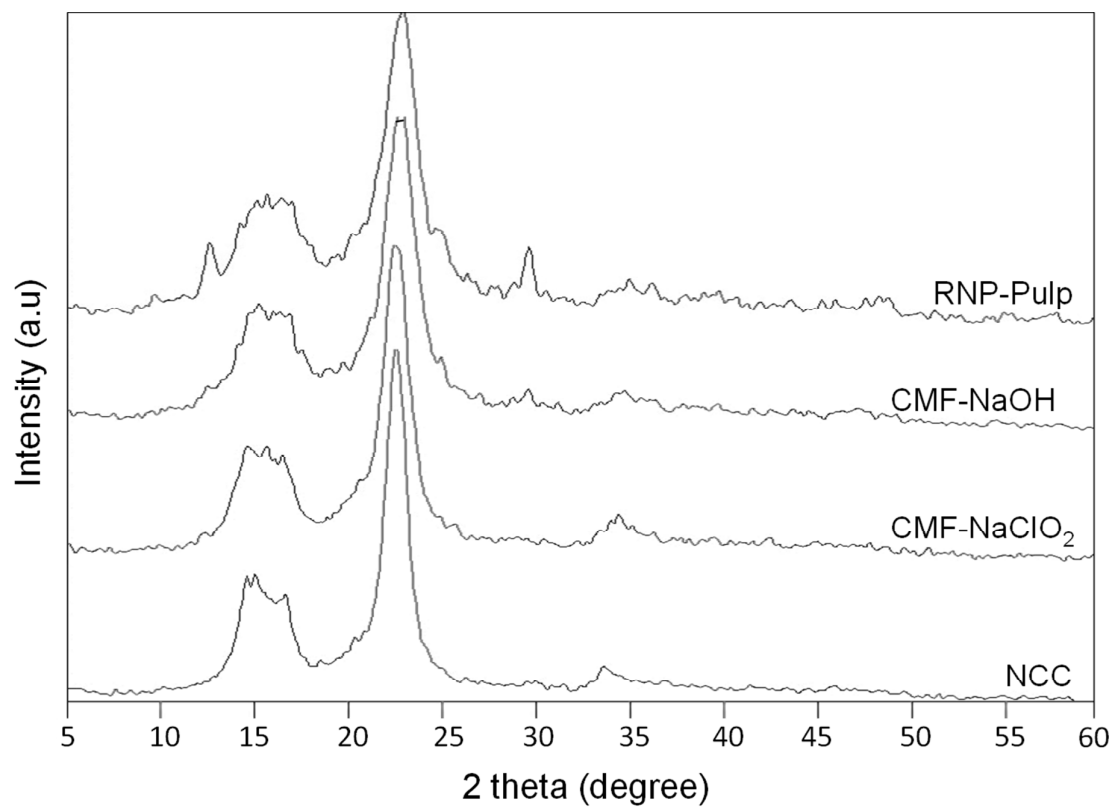


Fig 5: XRD pattern of RNP-pulp, CMF-NaOH, CMF-NaClO₂, and NCC

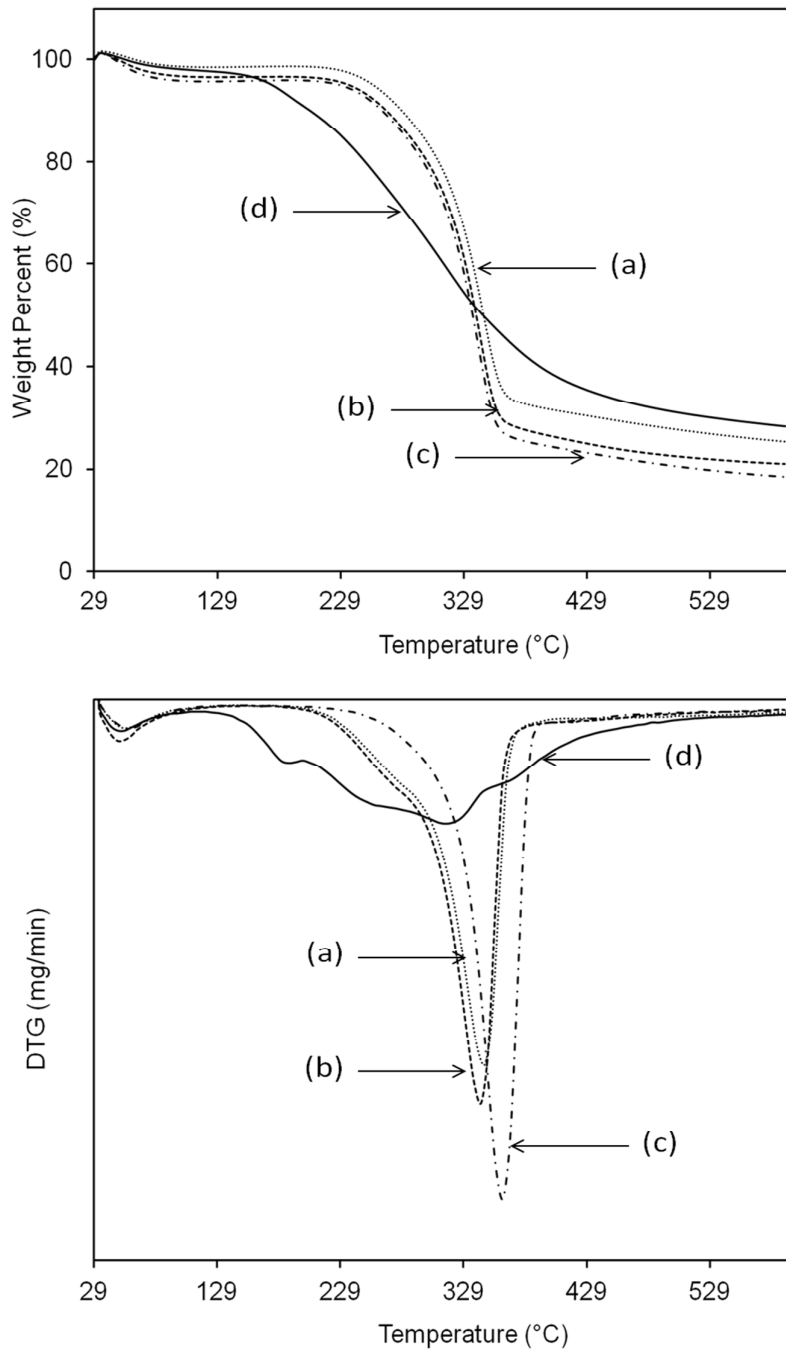


Fig 6: TGA and DTG curve of (a) CMF- NaClO_2 , (b) CMF- NaOH , (c) RNP-pulp and (d) nanocrystalline cellulose.